V-Proportion: A Method Based on the Voronoi Diagram to Study Spatial Relations Between Neuronal Mosaics

Oscar M. Mozos* Jose A. Bolea† Eduardo Fernandez‡ Peter K. Ahnelt§

Abstract

The study of the spatial relations between neural populations has shown its importance to investigate possible constrains or connectivities between different cell types. In this paper we present the application of the Voronoi diagram to detect possible spatial relations between cells.

1 Introduction

The study of the spatial relations between neural populations has shown its importance to investigate possible constrains or connectivities between different cell types. A positive spatial dependencies between two different populations of neurons may be an indicator of some connection patterns between them [1, 5, 4, 2]. The spatial information is also helpful to study dependencies during development [10].

Different methods to study spatial relations between different cell populations have been proposed in the past. The work in [14] extends the density recovery profile method [17] to study interdependences between different S-cone cells. In [7], the author uses the K-function [16] to analyze the spatial relation between *on* and *off* cells in the eye retina. The same cells are studied in [8] by fitting a bivariate pairwise interaction model in the data. Spatial relations between beta cells are studied in [20] using K-nearest neighbor histograms. This data was also analyzed in [19] using the J-function.

This paper introduces a method to study spatial relations between two cell populations. The key idea is to calculate the Voronoi diagram of one of the populations, and then study the spatial distribution of cells in the second population inside the polygons of the diagram. Using polygonal areas around neural cells is a realistic approximation, since neurons present different irregularities in their structure [11]. In this work we extend preliminary ideas and results presented in [2].

2 The Voronoi Diagram

The Voronoi diagram [3] is one of the most useful geometrical constructions to study point patterns because it provides all the information needed to study the proximity relations in a set of points.

We define a Voronoi diagram as follows. Let $P = \{p_1, p_2, \ldots, p_n\}$ be a set of points in the two dimensional Euclidean plane. We refer to these points as *reference points*. Now we assign every other point in the plane to its nearest reference point p_i. This process creates a tessellation of the plane into (sometimes unbounded) convex polytopes, also called Voronoi polygons. Let $V(p_i)$ be the Voronoi polygon corresponding to reference point p_i, then all the points inside this polygon are at least as close to p_i as to any other reference point p_j

$$V(p_i) = \{p \mid d(p_i, x) \leq d(p_j, x),\ \forall p_i \neq p_j\},$$

*Department of Computer Science and System Engineering, University of Zaragoza, Spain. ommozos@unizar.es
†Bioengineering Institute, Miguel Hernandez University, Spain
‡Bioengineering Institute, Miguel Hernandez University, Spain
§Department of Physiology, Medical University of Vienna, Austria

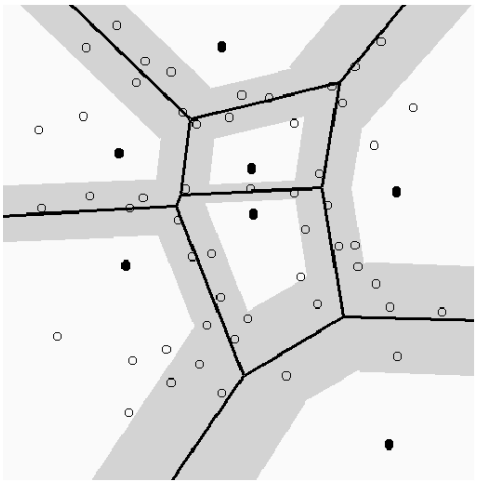

Figure 1: Example of a Voronoi diagram (black lines) for a set of reference points (black circles). Bands around the edges of the Voronoi diagram are shown in gray. In this particular case $\delta = 0.29$, indicating the 29% of the distance between a Voronoi edge and its closest reference point.

with $d(x, y)$ representing the Euclidean distance function.

The edges of the Voronoi regions form the Voronoi diagram $V(P)$ of a the reference points set. Note that a point on the edges of the Voronoi diagram has two nearest neighbors and each vertex has at least three. An example of a Voronoi Diagram is shown in Figure 1.

3 The V-Proportion Measurement

Let's suppose we want to study the possible spatial interaction between two cell populations denoted as P and Q. In principle, we want to study whether the cells in the Q population have a tendency to be far from the cells in P. In this case, the average density of q-cells will be higher near the edges of the Voronoi diagram than in the surrounding of the p-cells (Voronoi polygons). An example is given in Figure 1, where p-cells are shown as black circles (reference points), and q-cells as white circles.

To quantify this far concept we construct bands around the edges of the Voronoi diagram with a specified width (gray areas in Figure 1). If both populations, P and Q are spatially independent, then the average density of q-cells should be the same in any region inside the Voronoi polygons. If there exists an inhibition between the P and Q populations, then the density of q-cells should be higher in the band zone. On the contrary, if there exists an attraction, then the density of q-cells should be higher close to p-points and far from the edges. A way to quantified these spatial relations can be obtaining by looking at the relative proportion between q-cells inside the bands n_b and the total number of q-cells inside the Voronoi polygons n_{vp}

$$\text{V-proportion} = \frac{n_b}{n_{vp}}. \tag{1}$$

If the measured V-proportion is higher than expected, then there should be more points inside the bands, suggesting a negative correlation. If the measured V-proportion is lesser than expected, then a positive correlation can be assumed.

An important issue in this method is the determination of the band widths. To determine this value, we have to take into account that distances between the reference points p_i and the edges of their respective Voronoi polygon $V(p_i)$ are usually different for each reference point. As a result, polygons with different sizes and shapes are obtained. This effect mainly appears in neuron populations, and it is due to dendritic tree irregularities [11, 2]. To solve this problem a non-fixed value for the width in each band is used. This value is represented by the parameter δ, $0 < \delta < 1$, and indicates the proportion of the distance between each of the edges of $V(p_i)$ and the reference point p_i . As an example, a value

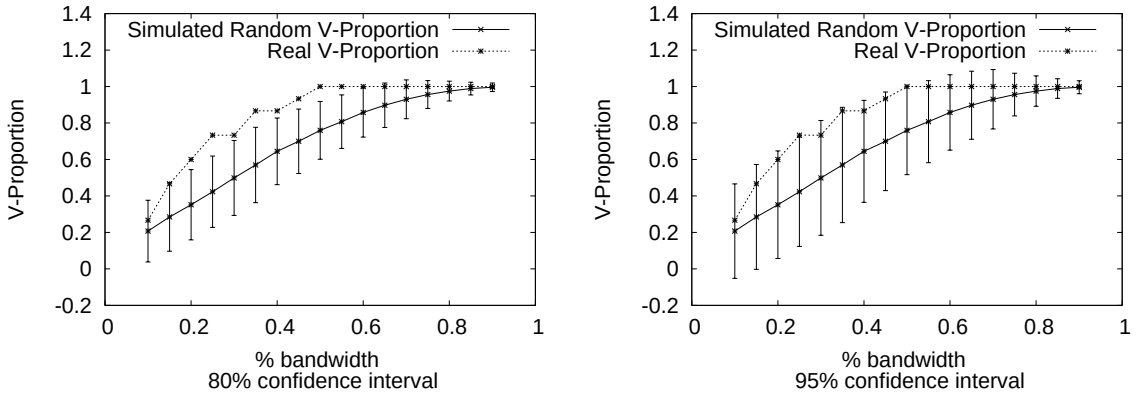

Figure 2: The plots shows the V-proportion for the populations of Figure 1 in comparison with the simulated ones. The V-proportion is calculated for different band widths. Errors bars on the left plot are at the 80% confidence interval, while on the right plot are at the 95% confidence interval.

of $\delta = 0.29$ means that the width of the band for one edge must be 29% of the distance between that edge and the reference point (Figure 1).

It remains to explain how to quantify the expected values to be compared with Expression 1. To test the significance of the V-proportion, we use a Monte Carlo test procedure. This involves generating a set of two random and independent patterns, each with the same number of points as the two empirical populations P and Q, and in a study area identical to that of these patterns. We repeat the generation N times for each δ, and then the mean and the standard deviation of the V-proportion for each simulation are calculated. The resulting plot is compared with the V-proportion obtained with the two real P and Q populations. Whenever the real V-proportion raises above the random equivalent simulation, then we can assume a negative interaction between patterns, that is, P inhibits Q. If the real V-proportion is below the simulated one, then a clustering process occurs in which P cells attract Q cells. If the real V-proportion is close to the simulated one, we can not assume any spatial interaction between the two populations.

Finally, an important problem when working with point populations is the edge effect. Typically, the observation of the two point patterns is restricted to a regular sampling window, while usually the patterns extend beyond the window. Furthermore, the Voronoi polygons on the boundary of the area are open because they have no neighboring points in those directions. This edge effect affects the sense of bands in the Voronoi polygons adjacent to the edges. In our case, we solve this problem by removing the Voronoi polygons intersecting the edges of the sampling area (open polygons). Similar approaches have been applied in other works for studying cell mosaics [13, 9]. Although this heuristic reduces the total number of points used for the study, we think the results represent the spatial relations in a more reliable manner.

An example of this process is shown in Figure 2. Here the V-proportion for the populations in Figure 1 is calculated, where P cells correspond to black circles and Q cells to white ones. We generated 100 simulations for the two populations. The simulations points were distributed randomly in the space. As both plots in Figure 2 indicate, the V-proportion of the two populations is always above the simulated values. This indicates that the Q population tends to be inhibited by the P population. In the left plot of Figure 2, we can see that the V-proportion values fall most of the time above the 80% confidence interval. That means that the negative interaction between cells is significant at the 0.20 level. However, this difference is no more significant at the 0.05 level (95% confidence interval) as shown in the right plot in Figure 2.

4 Results

This section presents experimental results that validate our approach. We first show experiments in simulated populations that follow different spatial distributions. We then study the spatial relations

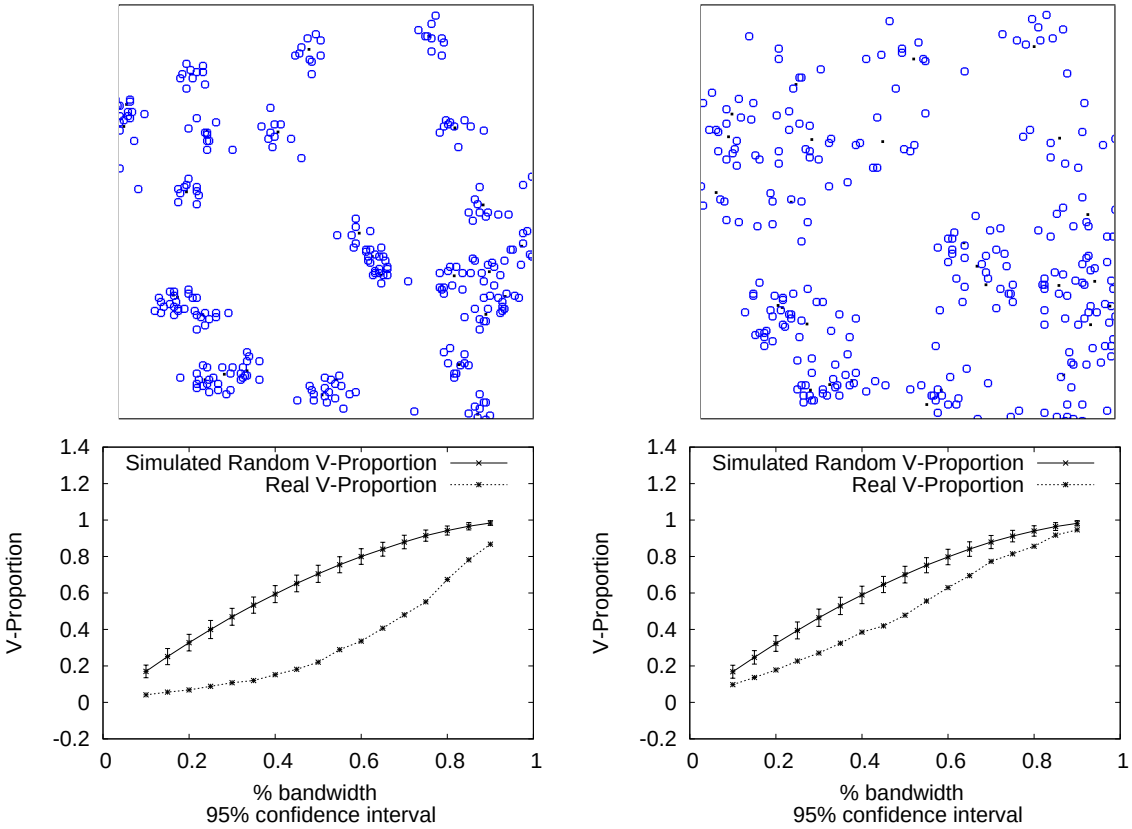

Figure 3: Two Poisson clusters (upper images) with different values of σ^2 in pixel units (left $\sigma^2 = 25$, right $\sigma^2 = 100$). The area of the original image was 300×300 pixels. P points are shown in black, whereas Q points are depicted in blue circles. Both clustering behaviors are clearly detected.

between real cell populations that have been previously studied in the literature.

4.1 Simulated Populations

In the following experiments we generated pairs of point patterns following a mathematical probability distribution, and then we calculated their V-proportion. As explained in Section 3, we use two set of populations. The P population will be the reference one, and the Q population will be the one to study its spatial distribution.

We first study clusters behaviors of Q points with respect P points To generate the both patterns, we simulate the Poisson cluster process presented in [15, 6] as follows. Each parent point p is generated following a bidimensional Poisson process. For each p-point, we generate a set of q offspring points. The positions of the q-point relative to their parents are independent and identically distributed according to a bidimensional normal distribution. Details on the simulations can be found in [18]. We generate different pairs of P and Q populations with 50 and 300 points respectively. The points are contained in an image area of 300×300 pixels. For each pair of populations, we change the variance σ^2 of the offsprings q-points. Example simulations are shown in Figure 3 together with their V-proportions. In these plots the interval confidence represented by the error bars is of 95%. As we can see the clusters are detected by the V-proportion plots. A way to determine the level of clustering could be calculating the area under the curve between the random simulations and the real patterns.

In a second simulation we generate a Q population in which each point can not be closer to a P point less than a certain radius (80 pixels). Details on the simulation are found in [12]. Results are shown in Figure 4. The plot clearly indicates the negative correlation between the populations at the 95% confidence interval. In a third simulation, we generate independent Poisson processes for both P and Q populations. Part of the populations and V-proportions are shown in Figure 5. The plot

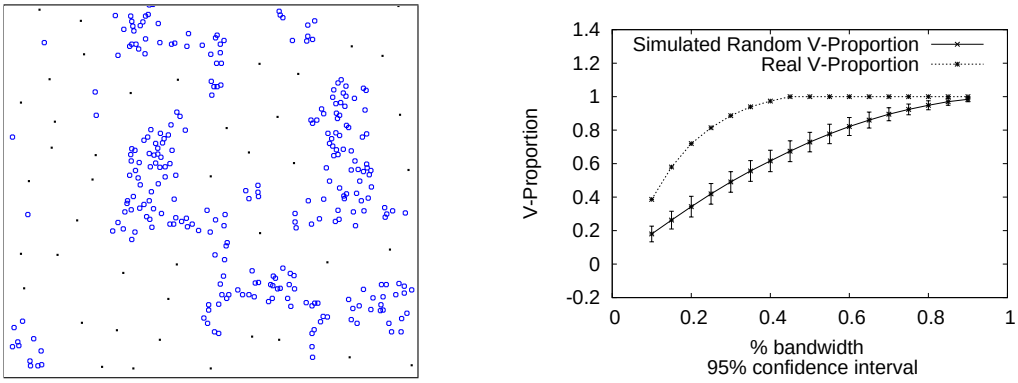

Figure 4: The left image depicts the populations P and Q generated following a repulsion model [12]. The right plot clearly indicates a negative spatial relation between both populations.

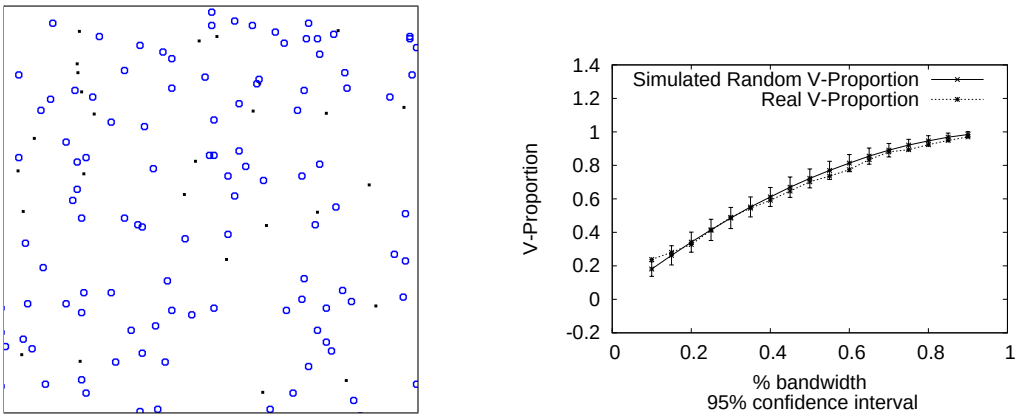

Figure 5: The left image depicts the populations P and Q generated following two independents Poisson point processes. The right plot does not indicate any spatial relation between both populations.

correctly indicates that we can not describe any positive or negative spatial relation between the two populations.

In summary, the previous experiments clearly show that the V-proportion value is able to detect cluster and repulsion behaviors, as well as the lack of them.

4.2 V-proportion in real cell populations

In this section we apply the V-proportion measurement to real populations of cells. In addition, we compare the results with previous works analyzing the same patterns.

4.2.1 Beta cells in the cat retina

The left image in Figure 6 depicts a pattern of beta-type ganglion cells in the retina of a cat [20]. Beta cells are associated with the resolution of fine detail in the cat's visual system. They can be classified as *on* or *off*, depending on the branching level of their dendritic tree in the inner plexiform layer. Analysis of the spatial pattern provides information on the cat's visual discrimination. In particular, independence of the *on*- and *off*-components would strengthen the assumption that there are two separate channels for *brightness* and *darkness*. More details can be found in [20].

In [20] this pattern is investigated using histograms of nearest-neighbor distances (ignoring edge effects). To test independence of the *on* and *off* patterns, a random translation of the *off*-component was superimposed on the *on*-component, and the resulting nearest-neighbor histogram was compared

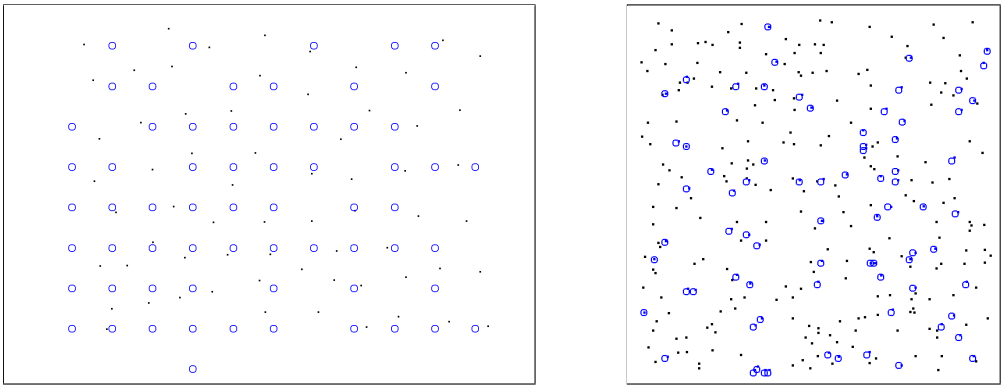

Figure 6: the left image shows the superimposed patterns of *on* and *off* cells in the cat retina. In the right image we can see the cell nuclei of the hamster's kidney.

with the original one by a sign reversal test. The authors in [20] concluded that both types of beta cells form a regular lattice, which are superimposed independently. This data was also analyzed in [19] using the J-function with a result greater than 1, which confirms conclusions of [20]. Our results using the V-proportion are shown in the top plots of Figure 7. Using an confidence interval of 95% we cannot assume a significant negative spatial relation between *on* and *off* cells. However, at a confidence interval of 80% we can see a slightly negative repulsion. This small negative effect was not indicated in previous works analyzing this pattern.

4.2.2 Hamster tumor

The right image in Figure 6 shows the positions of cell nuclei in approximately $0.25mm$ square histological sections of tissue from laboratory-induced metastasising lymphoma in the kidney of a hamster. Two types of cells are distinguished: 77 pyknotic nuclei corresponding to dying cells, and 226 nuclei arrested in metaphase. In [6] this pattern was studied and the random labeling hypothesis using the K-function was accepted. Results in [19] agreed on the random hypothesis using the J-function. In our analysis, we support the independence between both populations at the 80% and 95% confidence level, as shown in the bottom plots in Figure 7.

5 Conclusion

This paper introduced a method to evaluate spatial relations between different neural cells. Our approach is based on the Voronoi diagram and considers the relation between the density of points inside Voronoi polygons and bands around it edges. The method has been tested in simulated populations as well as in real ones. Results demonstrate that our measurement can be used to detect different spatial relations between populations, such as repulsions, attractions or none of them.

References

[1] P.K. Ahnelt and H. Kolb, Horizontal cells and cone photoreceptors in primate retina: a Golgi-light microscopic study of spectral connectivity, *The Journal of Comparative Neurology*, vol. 343, pp. 387–405, May 1994.

[2] P.K. Ahnelt, E. Fernandez, O. Martinez, J.A. Bolea, and A. Kueber-Heiss, Irregular S-cone mosaics in felid retinas. Spatial interaction with axonless horizontal revealed by cross-correlation, *Journal of the Optical Society of America A*, vol. 17(3), pp. 580–588, March 2000.

[3] M. de Berg, O. Cheong, M. van Kreveld, and M. Overmars, *Computational Geometry: Algorithms and Applications*, Springer-Verlag, third edition, 2008.

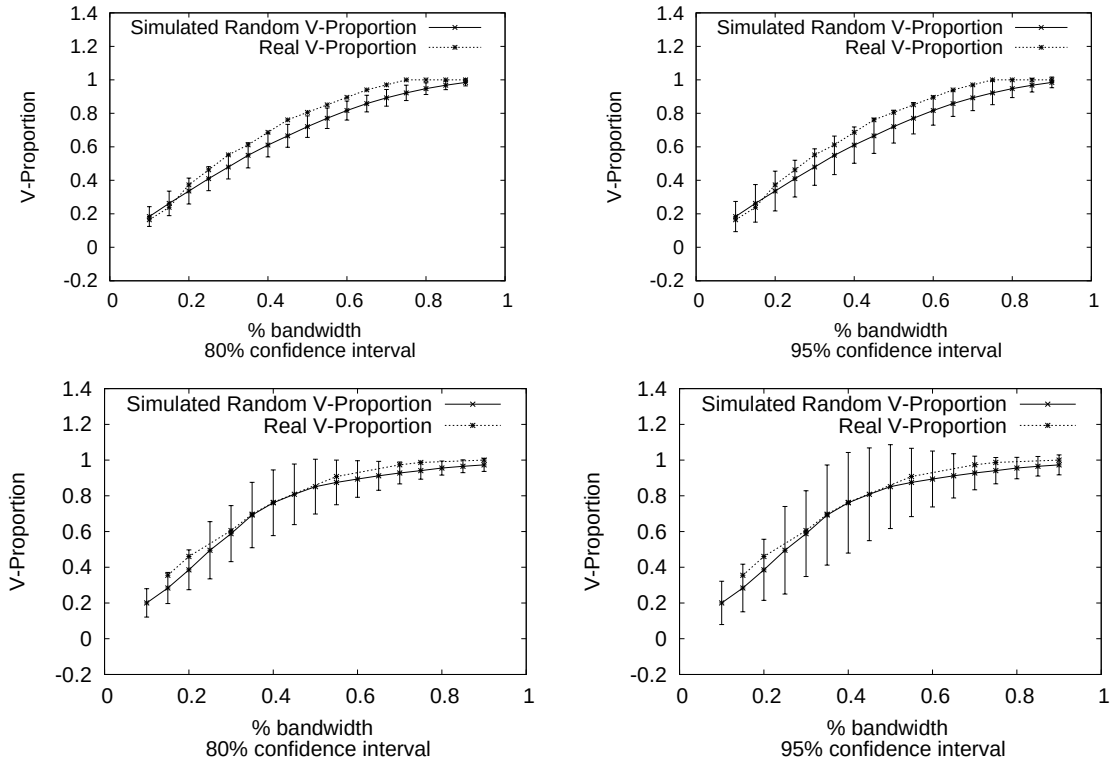

Figure 7: The top plots depicts the V-Proportion for the superimposed patterns of *on* and *off* cells in the cat retina (left image in Figure 6). The repulsion between populations is slightly significant at the 80% confidence level. However, this negative relation is not significant at the 95% confidence level. The bottom plots present the V-proportion for the nuclei of a hamster (right image in Figure 6). Both plots do not indicate neither positive or negative spatial relations between the two cell populations.

[4] T.L. Chan, and U. Gruenert, Horizontal cell connections with short wavelength-sensitive cones in the retina: a comparison between New World and Old World primates, *The Journal of Comparative Neurology*, vol. 393(2), pp. 196–209, April 1998.

[5] D.M. Dacey, B.B. Lee, D.K. Stafford, J. Pokorny, and V.C. Smith, Horizontal cells of the primate retina: cone specificity without spectral opponency, *Science*, vol. 271(5249), pp. 656–659, February 1996.

[6] P. Diggle, *Statistical analysis of spatial point patterns*, Academic Press 1983.

[7] P.J. Diggle, Displaced amacrine cells in the retina of a rabbit: analysis of a bivariate spatial point pattern, *Journal of Neuroscience Methods*, vol. 18(1-2), pp. 115–125, October 1986.

[8] P.J. Diggle, S.J. Eglen, and J.B. Troy, *Case Studies in Spatial Point Process Modelling*, ch. Modelling the bivariate spatial distribution of amacrine cells, pp. 215–233, Springer, 2006.

[9] C. Duyckaerts, and G. Godefroy, Voronoi tessellation to study the numerical density and the spatial distribution of neurones, *Journal of Chemical Neuroanatomy*, vol. 20(1), pp. 83–92, October 2000.

[10] S.J. Eglen, Development of regular cellular spacing in the retina: theoretical models, *Mathematical Medicine and Biology*, vol. 23(2), pp. 79–99, June 2006.

[11] E. Fernandez, J. A. Bolea, G. Ortega, and E. Louis, Are neurons multifractals?, *Journal of Neuroscience Methods*, vol. 89(2), pp. 151–157, July 1999.

[12] E. Fernandez and N. Cuenca and J. De Juan, A compiled BASIC program for analysis of spatial point patterns: application to retinal studies, *Journal of Neuroscience Methods*, vol. 50(1), pp. 1–15, October 1993.

[13] L. Galli-Resta, E. Novelli, Z. Kryger, G.H. Jacobs, and B.E. Reese, Modelling the mosaic organization of rod and cone photoreceptors with a minimal-spacing rule, *The European Journal of Neuroscience*, vol. 11(4), pp. 1461–1469, April 1999.

[14] N. Kouyama, and D.W. Marshak, The topographical relationship between two neuronal mosaics in the short wavelength-sensitive system of the primate retina, *Visual Neuroscience*, vol. 14(1), pp. 159–167, January 1997.

[15] J. Neyman and E.L. Scott, A statistical approach to problems of cosmology, *Proceedings of the Royal Society of London. Series B (Methodological)*, vol. 20(1), pp. 1–43, 1958.

[16] B.D. Ripley, The Second-Order Analysis of Stationary Point Processes, *Journal of Applied Probability*, vol. 13(2), pp. 255–266, June 1976.

[17] R.W. Rodieck, The density recovery profile: a method for the analysis of points in the plane applicable to retinal studies, *Visual Neuroscience*, vol. 6(2), pp. 95–111, February 1991.

[18] S. M. Ross, *Simulation*, Academic Press, 1997.

[19] M.N.M. van Lieshout, and A.J. Baddeley, Indices of Dependence Between Types in Multivariate Point Patterns, *Scandinavian Journal of Statistics*, vol. 26, pp. 511–532, 1999.

[20] H. Wassle, B. B. Boycott, and R.-B. Illing, Morphology and mosaic of on- and off-beta cells in the cat retina and some functional considerations, *Proceedings of the Royal Society of London. Series B (Biological Sciences)*, vol. 212(1187), May 1981.